Fujishim Y, et al	Efficacy of liraglutide, a glucagon-like peptide-1 (GLP-1) analogue, on body weight, eating behavior, and glycemic control, in Japanese obese type 2 diabetes	Cardiovasc Diabetol	11	107	2012

【３】研究成果の刊行物・別刷

Biochemical and Biophysical Research Communications 417 (2012) 1107–1112

Contents lists available at SciVerse ScienceDirect

Biochemical and Biophysical Research Communications

journal homepage: www.elsevier.com/locate/ybbrc

Rat glucagon receptor mRNA is directly regulated by glucose through transactivation of the carbohydrate response element binding protein

Katsumi Iizuka [a,b,*], Reiko Tomita [a], Jun Takeda [a], Yukio Horikawa [a]

[a] Department of Diabetes and Endocrinology, Graduate School of Medicine, Gifu University, Gifu 501-1194, Japan
[b] Gifu University, University Hospital Center for Nutritional Support and Infection Control, Gifu 501-1194, Japan

ARTICLE INFO

Article history:
Received 6 December 2011
Available online 16 December 2011

Keywords:
Carbohydrate response element binding protein (ChREBP)
Glucagon receptor
cAMP
G-box
Carbohydrate response element (ChoRE)
Glucagon

ABSTRACT

The glucagon receptor (*Gcgr*) is essential for maintaining glucose homeostasis in the liver and for stimulating insulin secretion in pancreatic β-cells. Glucose induces rat *Gcgr* mRNA expression; however, the precise mechanism remains unknown. We previously have studied the role of the carbohydrate response element binding protein (ChREBP), a glucose-activated transcription factor, in the regulation of glucose-stimulated gene expression. The G-box has previously been reported to be responsible for glucose regulation of *Gcgr* mRNA expression. The G-box comprises two E-boxes separated by 3 bp, which distinguishes it from the carbohydrate response element (ChoRE), which has 5-bp spacing between the two E-boxes. In the rat *Gcgr* promoter, a putative ChoRE (−554 bp/−538 bp) is localized near the G-box (−543 bp/−529 bp). In rat INS-1E insulinoma cells, deletion studies of the rat *Gcgr* promoter show that ChoRE is a minimal glucose response element. Moreover, reporter assays using a pGL3 promoter vector, which harbors ChoRE and chromatin immunoprecipitation assays reveal that ChoRE is a functional glucose response element in the rat *Gcgr* promoter. Furthermore, In contrast, glucagon partly suppresses glucose-induced expression of *Gcgr* mRNA. Thus, ChREBP directly regulates rat *Gcgr* expression in INS-1E cells. In addition, negative feedback looping between ChREBP and GCGR may further contribute to the regulation of glucose-induced gene expression.

1. Introduction

Type 2 diabetes mellitus (T2DM) has become a serious health problem worldwide. T2DM is characterized by a decrease in insulin secretion caused by β-cell dysfunction and death and an increase in insulin resistance [1]. The role of glucagon in this process is the focus of much attention in current research [2–4]. In the liver, the actions elicited by glucagon are essential for maintaining a euglycemic state under normal physiological conditions [2–4]. On the other hand, hyperglucagonemia is associated with hyperglycemia and diabetes under pathophysiological conditions [2–4]. A state of chronic hyperglucagonemia is correlated with excess hepatic glucose production and hyperglycemia in diabetic patients [2–4]. Indeed, experimental suppression of hyperglucagonemia has been shown to correct postprandial hyperglycemia in diabetic patients [4]. Similarly, antagonism of the glucagon receptor gene (*Gcgr*) and its deletion improve glucose tolerance in genetically obese mice [5–7]. Interestingly, *Gcgr* mRNA expression is positively regulated by glucose both in vitro and in vivo [8,9]. Elucidation of the mechanisms underlying glucose-induced expression of *Gcgr* mRNA in the liver and pancreatic islets should be of significant value in broadening the approaches to improving effective glycemic control in patients with T2DM [2–4].

We have previously studied the role of the carbohydrate response element binding protein (ChREBP), a glucose-activated transcription factor, in the regulation of glucose-induced gene expression in the liver [10–17]. *Chrebp* mRNA and *Gcgr* mRNA are generally expressed in the same tissues, including liver, kidney, intestinal smooth muscle, brain, adipose tissue, heart, and pancreatic islet β-cells [10,18]. ChREBP binds to the carbohydrate response element (ChoRE) to induce lipogenic gene expression [11–13,16]. ChoRE is composed of two tandem E-boxes separated by 5 bp [10,19–21]. Two CACGTG motifs, separated only by 5 bp, can induce glucose-stimulated gene transcription [19]. It has also been reported that a G-box composed of two E-box motifs separated by 3 bp forms a glucose response element in the rat *Gcgr* promoter [8,22,23]. However, whether this G-box is functional is questionable for the following reasons: (1) the rat G-box is composed of two E-boxes separated by only 3 bp [22,23], (2) the sequence of the rat G-box differs from that of the mouse G-box [22–23], and (3) deletion of one E-box does not affect luciferase activities [22,23]. Since glucagon suppresses ChREBP transactivity through the cAMP-dependent protein kinase (PKA) pathway in the liver [10,24], we considered that ChREBP directly regulates

* Corresponding author. Address: Department of Diabetes and Endocrinology, Graduate School of Medicine, Gifu University, Gifu 501-1194, Japan. Fax: +81 58 230 6376.
E-mail address: kiizuka@gifu-u.ac.jp (K. Iizuka).

0006-291X/$ - see front matter © 2011 Elsevier Inc. All rights reserved.
doi:10.1016/j.bbrc.2011.12.042

Gcgr mRNA expression or that glucagon regulates *Gcgr* mRNA expression through inhibition of ChREBP transactivity.

In this study, we identify a functional ChoRE in the *Gcgr* promoter and a closed loop system between glucose (ChREBP) and glucagon (GCGR) signaling. This mechanism of negative feedback between glucose and glucagon suggests novel strategies for treating fasting and postprandial hyperglycemia in T2DM patients.

2. Materials and methods

2.1. Materials and cell culture

The rat insulinoma cell line, INS-1E, (a gift by C.B. Wollheim, University of Geneva) was maintained under 5% CO_2 at 37 °C in Roswell Park Memorial Institute (RPMI)-1640 medium (Invitrogen, Carlsbad, CA) supplemented with antibiotics, pyruvate, mercaptoethanol, and 15% fetal calf serum, as previously described [25]. Glucagon was purchased from Fuji Seiyaku Kohgyo (Toyama, Toyama, Japan).

2.2. RNA extraction, cDNA synthesis, and real-time reverse transcriptase PCR quantification

Cells were preincubated in RPMI media with 2.5 mM glucose for 12 h. After 12-h incubation with various glucose concentrations, cells were collected and used for RNA extraction, cDNA synthesis, and real-time reverse transcriptase PCR (RT-PCR) analysis, as described previously [12–15]. Relative mRNA levels were determined by real-time RT-PCR and normalized to rat RNA polymerase II (Pol) mRNA. The real-time PCR primers used were as follows: Gcgr-Probe, 5′-FAM-TGCCCCCACCTACTGAGCTGGTCTG-TAMRA-3′; Gcgr-F, 5′-GCCACCACAACCTAAGCCT-3′; Gcgr-R, 5′-GGCCAGCAGGAGTACTTGTC-3′; Pol-Probe, 5′-CAACTGGTGACAGCAAGGTGGTCCTCC-3′; Pol-F, 5′-CGGGAAGTGCTCAGGGTCA-3′; Pol-R, 5′-GAGGGAAGGCGAGGGTTGA-3′. Similarly, after preincubation with 2.5 mM glucose for 12 h, cells were incubated in media with 25 mM glucose for 3, 6, and 12 h, when they were collected for RNA extraction, cDNA synthesis, and real-time RT-PCR analysis, as described previously [14–17]. To test the effect of glucagon, cells were incubated in media including 2.5 or 25 mM glucose with and without final concentrations of 10^{-8} M glucagon for 8 h, when they were collected for further analysis of real time quantitative PCR, as described previously [14–17].

2.3. Construction of plasmids and adenovirus vectors

We used pcDNA-daChREBP, Ad-daChREBP, Ad-dnMlX, and pRL-SV40 vectors, as previously described [14–17]. A series of pGL3-promoter vectors were constructed as follows: three fragments, G-box (−548/−524 bp), ChoRE + 6 (−559/−527 bp), ChoRE + 3 (−559/−530 bp), ChoRE (−559/−533 bp), ChoRE-3 (−559/−536 bp), and ChoRE-7 (−559/−540 bp) were cloned into pGL3 vectors upstream of the TK promoter. All plasmid and adenovirus vectors were verified by sequencing analysis.

2.4. Treatment with recombinant adenovirus

INS-1E cells were cultured in 6-well plates in 2 ml RPMI. Adenovirus bearing dominant-active ChREBP (daChREBP) cDNA was used

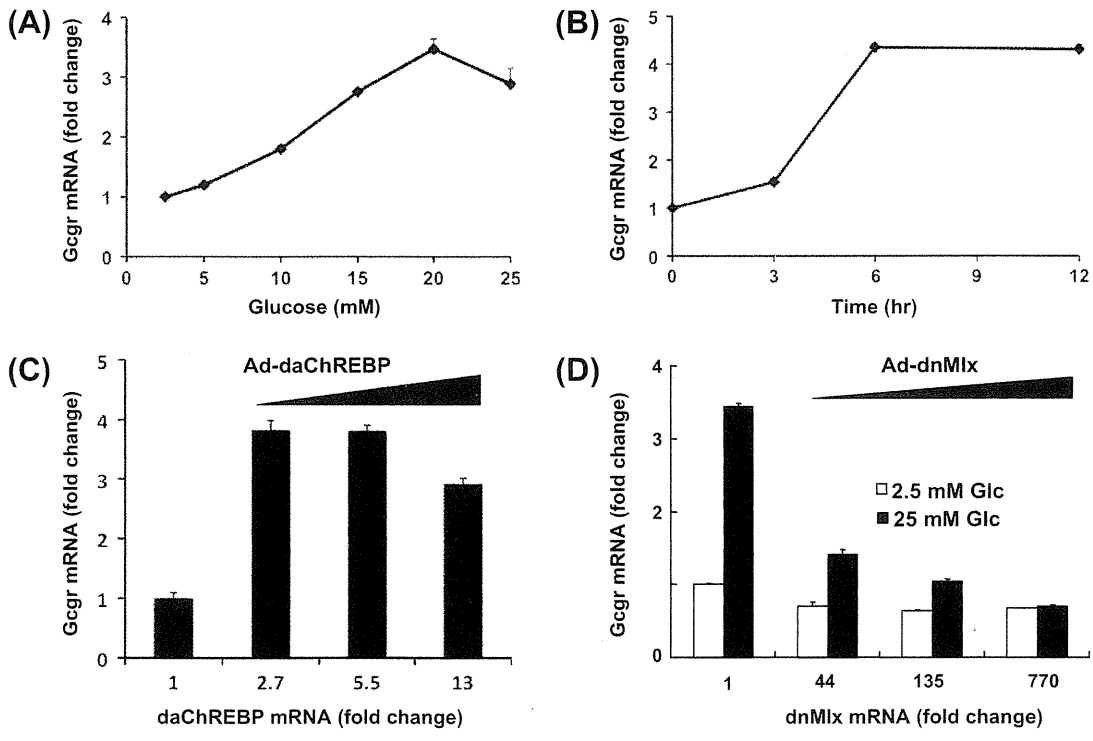

Fig. 1. Glucose induces rat *Gcgr* mRNA expression in a time- and dose-dependent manner. (A) Glucose induces rat *Gcgr* mRNA expression in a dose-dependent manner. INS-1 cells were cultured for 12 h in culture medium containing 2.5, 5.0, 10, 15, 20 or 25 mM glucose. Relative mRNA levels were determined by real-time RT-PCR and normalized to rat *RNA polymerase II* (*Pol2*) mRNA as the invariant control. The change in expression level of each normalized enzyme mRNA level was determined with reference to the value for INS-1 cells at 2.5 mM glucose, which was arbitrarily defined as 1. Data represent means ± S.D. (n = 3). (B) Glucose induces rat *Gcgr* mRNA expression in a time-dependent manner. INS-1 cells were cultured in RPMI media including 2.5 mM glucose for 12 h. Media were changed to RPMI media including 25 mM glucose and collected at the indicated hours for Taqman RT-PCR analysis. Data represent means ± S.D. (n = 3). (C) Adenoviral overexpression of dominant active ChREBP causes rat *Gcgr* mRNA expression in INS-1E cells. INS-1 cells were infected with 2, 10, and 50 m.o.i. of Ad-daChREBP for 2 h. After culture in RPMI media with 2.5 mM glucose concentration for 12 h, the cells were collected for Taqman RT-PCR analysis. Data represent means ± S.D. (n = 3). (D) Adenoviral overexpression of dominant negative Mlx (dnMlx) causes glucose-stimulated gene expression in INS-1E cells. INS-1 cells were infected with 2, 10, and 50 m.o.i. of Ad-dnMlx for 2 h. After culture in RPMI media with 2.5 mM glucose concentration for 12 h, the cells were incubated in media with 2.5 mM or 25 mM glucose for 4 h and collected for Taqman RT-PCR analysis. Adenovirus bearing green fluorescence protein (GFP) was used as internal control. Values represent means ± S.D. (n = 3). At most points, the error bars are too small to be shown.

to infect INS-1E cells for 2 h. The medium was then removed and the INS-1E cells were incubated in a fresh medium with 2.5 mM glucose for 18 h. Adenovirus bearing dominant-negative Mlx (dnMlx) was used to infect INS-1E cells for 2 h. The medium was then removed and the INS-1E cells were incubated in a fresh medium with 3 mM glucose for 12 h, following which the medium was again removed and the cells were incubated in a fresh medium with either 2.5 or 25 mM glucose for an additional 4 h. Adenovirus bearing green fluorescence protein (GFP) was used as internal control. Cells were then collected and used for RNA extraction, cDNA synthesis, and real-time RT-PCR analysis, as described previously [14–17].

2.5. Mammalian transfection and reporter assay

Rat INS-1 cells were cultured in 6-well plates in 2 ml RPMI without antibiotics. The cells were transfected with 4 μl of Lipofectamine® 2000 transfection reagent (Invitrogen, California, USA); 1.5 μg of either pGL3-G-box, pGL3-ChoRE + 6, pGL3-ChoRE + 3, pGL3-ChoRE, pGL3-ChoRE-3, pGL3-ChoRE-7, or pGL3-empty and 0.1 μg of pRL SV40 vector (Invitrogen, California, USA) [14–17]. After 24 h of incubation with either 2.5 mM or 25 mM glucose, the cells were collected and luciferase activity was measured using the Dual-Luciferase® reporter assay system (Promega, Madison, WI, USA) according to the manufacturer's protocol. To determine the glucose dependency of the rat *Gcgr* promoter, cells were transfected with 1.5 μg of pGL3-ChoRE and 0.1 μg of pRL SV40 vectors. After 24 h of incubation with various glucose concentrations, the cells were collected for measurement of luciferase activity. To determine the dose dependency of daChREBP overexpression in the rat *Gcgr* promoter, cells were transfected with 0.5 μg of pGL3-ChoRE, 0.1 μg of pRL SV40 vectors, and 1.0 μg of pcDNA6.2 empty vector and pcDNA-daChREBP vector to adjust total DNA. After 24 h of incubation with either 2.5 mM or 25 mM glucose, the cells were collected for the measurement of luciferase activity. Similarly, after transfection with 1.5 μg of pGL3-ChoRE and 0.1 μg of pRL SV40 vectors, the cells were incubated in media with either 2.5 mM or 25 mM glucose containing 10^{-8} mM glucagon for 24 h.

2.6. Chromatin immunoprecipitation assay

A chromatin immunoprecipitation (ChIP) assay was performed with anti-ChREBP antibodies (Novus Biologicals, Littleton, CO) on formaldehyde cross-linked hepatocytes using Magna ChIP G beads (Millipore, Temecula, CA). INS-1E cells were precultured in 10-cm culture dishes with RPMI supplemented with 2.5 mM glucose, 15% FCS, and 100 μg/ml pen/strep for 12 h, followed by incubation in RPMI supplemented with 2.5 mM or 25 mM concentrations of glucose for 8 h. After incubation, 10% formaldehyde (270 μl) was added to the culture dishes and the cells were used for ChIP assays according to the manufacturer's protocol. The purified DNA was dissolved in Tris/EDTA (50 μl, pH 8.0) and used with gene-specific primers for PCR. A buffer solution and normal rabbit immunoglobulin G (Wako Chemical) were used as negative controls. Immunological chromatin samples were amplified by PCR using the primers as follows: Gcgr-CHIP-Probe, 5′-CCTCTGCTCCCACACACGGTGCA-3′; Gcgr-CHIP-F, 5′-CCTCAGAGCGGTCCATTATACC-3′; Gcgr-CHIP-R, 5′-TCTGGCTCCTGGGTGAAAGA-3′.

2.7. Data presentation and statistical methods

All data are expressed as mean ± standard deviation. The listed *n* values represent the number of single experiments performed

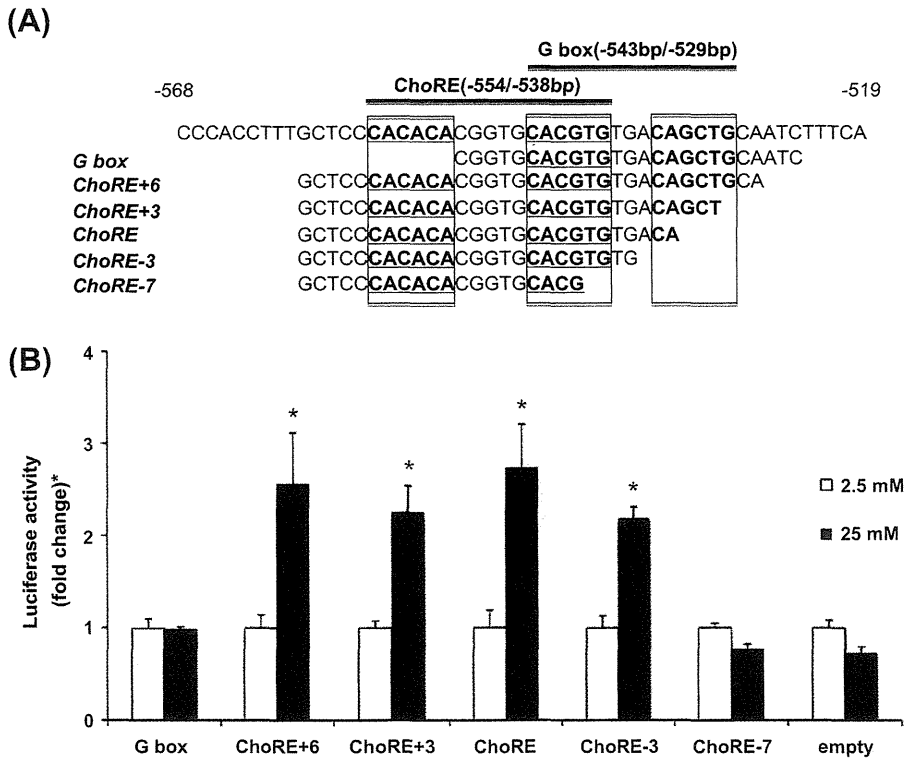

Fig. 2. ChoRE, but not G-box, is a functional glucose response element in the rat *Gcgr*. (A) Schematic representation of the G-box and the putative ChoRE in the rat *Gcgr* promoter. (B) Reporter analysis of deletion mutant of the ChoRE + 6 region (−559/−527 bp). Cells were co-transfected with 1.5 μg of pGL3 promoter vector inserted with either G-box, ChoRE + 6, ChoRE + 3, ChoRE, ChoRE-3, ChoRE-7, or empty vector and pRL SV40 (0.1 μg), and incubated in media with either 2.5 mM glucose or 25 mM glucose for 24 h. Cell lysates were collected for measurement of luciferase activities. Data represent means ± S.D. ($n = 6$). At most points, the error bars are too small to be shown.

(each experiment was duplicated). Comparison between the two groups was performed using the Student's *t*-test and that between multiple groups was performed using the Tukey–Kramer test. A *p*-value of <0.05 was considered statistically significant.

3. Results

3.1. Glucose stimulation and adenoviral overexpression of dominant active ChREBP causes an increase in rat glucagon receptor mRNA in INS-1E cells

We first ascertained whether glucose stimulation induces *Gcgr* mRNA expression in rat INS-1E cells. In INS-1E cells, glucose induced *Gcgr* mRNA expression in a dose- and time-dependent manner (Fig. 1A and B). Next, to clarify the role of the ChREBP/Mlx complex in *Gcgr* mRNA expression, we tested whether adenoviral overexpression of daChREBP induces *Gcgr* mRNA expression, and observed that adenoviral overexpression of daChREBP dose-dependently induced *Gcgr* mRNA expression in INS-1E cells (Fig. 1C). In accord with this, dnMlx, which acts as a decoy to antagonize ChREBP transactivity, inhibited glucose-induced *Gcgr* mRNA expression in INS-1E cells in a dose-dependent manner (Fig. 1D).

3.2. Identification of ChoRE in the rat glucagon receptor gene promoter

To determine the presence of ChoRE in the rat *Gcgr* promoter, we screened the region and found a putative ChoRE located between −554 and −538 bp, which differs from a G-box (from −543 to −529 bp) (Fig. 2A). To determine the functionality of this putative ChoRE, we performed a reporter assay using the pGL3 promoter vector inserted with deletion mutants of in the *Gcgr* promoter (Fig. 2B). In cells transfected with either pGL3-ChoRE-3, ChoRE, ChoRE + 3, ChoRE + 6 vectors, luciferase activities at 25 mM of glucose concentration were more than twice that at 2.5 mM glucose concentration (Fig. 2B). In contrast, luciferase activities in cells transiently transfected with either pGL3-ChoRE-7, G-box, or empty vectors were not increased by glucose stimulation (Fig. 2B). These data suggest that the rat *Gcgr* promoter contains a functional ChoRE between −554 and −538 bp.

3.3. Glucose and cotransfection of pcDNA-daChREBPP increases luciferase activities of pGL3-ChoRE in a dose-dependent manner

Glucose and cotransfection of pcDNA-daChREBP induced luciferase activities in pGL3-ChoRE in a dose-dependent manner (Fig. 3A and B). In accord with this, ChIP assays using anti-ChREBP

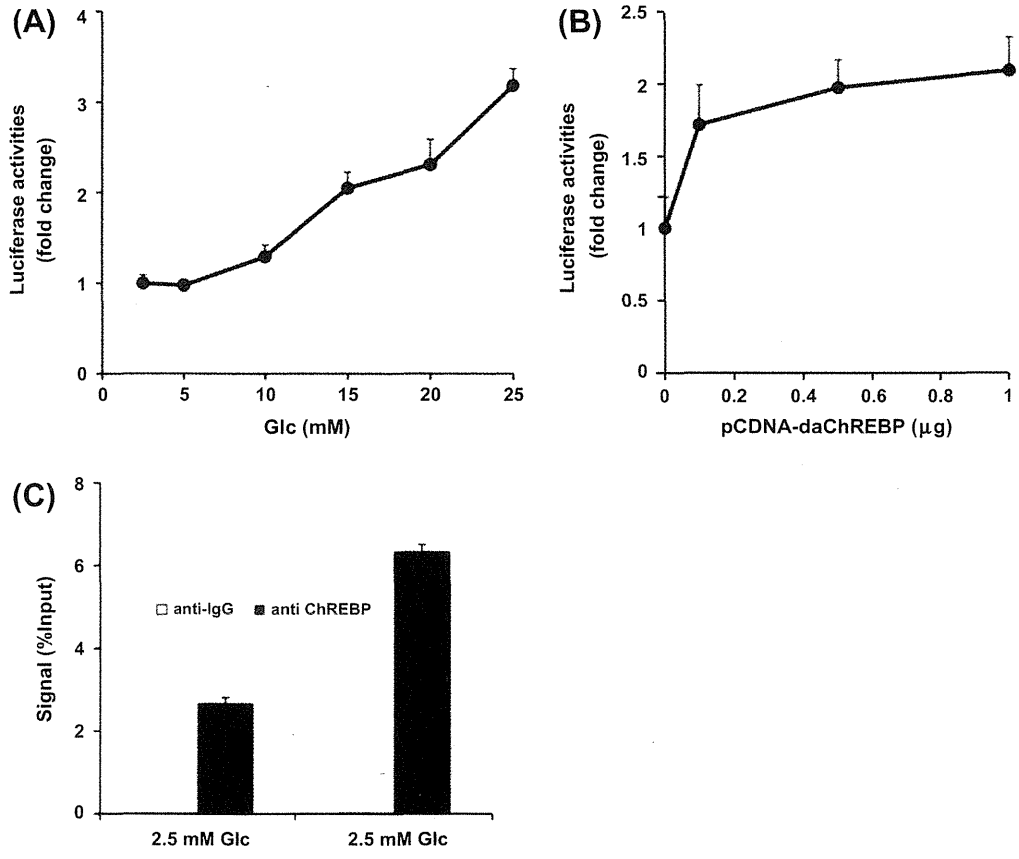

Fig. 3. ChoRE is a functional glucose response element to which ChREBP can bind. (A) Glucose dose-dependently induces luciferase activities in pGL3-ChoRE in INS-1E cells. INS-1 cells were cultured in six-well dishes and transfected with the series of pGL3-ChoRE vector (1.1 μg) and pRL-SV40 (0.4 μg) using Lipofectamine2000 (4 μl). After 24 h incubation in DMEM including several concentrations of glucose, luciferase activities were measured using Dual Luciferase assay kit. Data are mean ± S.D. ($n = 6$) of two independent experiments. At most points, the error bars are too small to be shown. (B) Cotransfection of pcDNA dominant active ChREBP (daChREBP) dose-dependently increases luciferase activities in pGL3-ChoRE in INS-1E cells. The pGL3-ChoRE vector (0.5 μg) and several concentrations of pcDNA daChREBP were cotransfected into INS-1E cells with pRL SV40 (0.1 μg). Total DNA was adjusted with pcDNA 6.2 empty vectors. The relative luciferase activity was expressed as an n-fold change with reference to the pcDNA 6.2 empty vector. Data are mean ± S.D. ($n = 6$) of two independent experiments. At most points, the error bars are too small to be shown. (C) ChIP assays reveal that ChREBP binding to ChoRE in 25 mM glucose is enhanced relative to the binding in 2.5 mM glucose. INS-1E cells were precultured in 10-cm culture dishes with RPMI supplemented with 2.5 mM glucose, 15% FCS, and 100 μg/ml pen/strep for 12 h, followed by incubation in RPMI supplemented with 2.5 mM or 25 mM concentrations of glucose for 8 h. After incubation, 10% formaldehyde (270 μl) was added to the culture dishes and the cells were used for ChIP assays according to the manufacturer's protocol. Data represent means ± S.D. ($n = 3$). At most points, the error bars are too small to be shown.

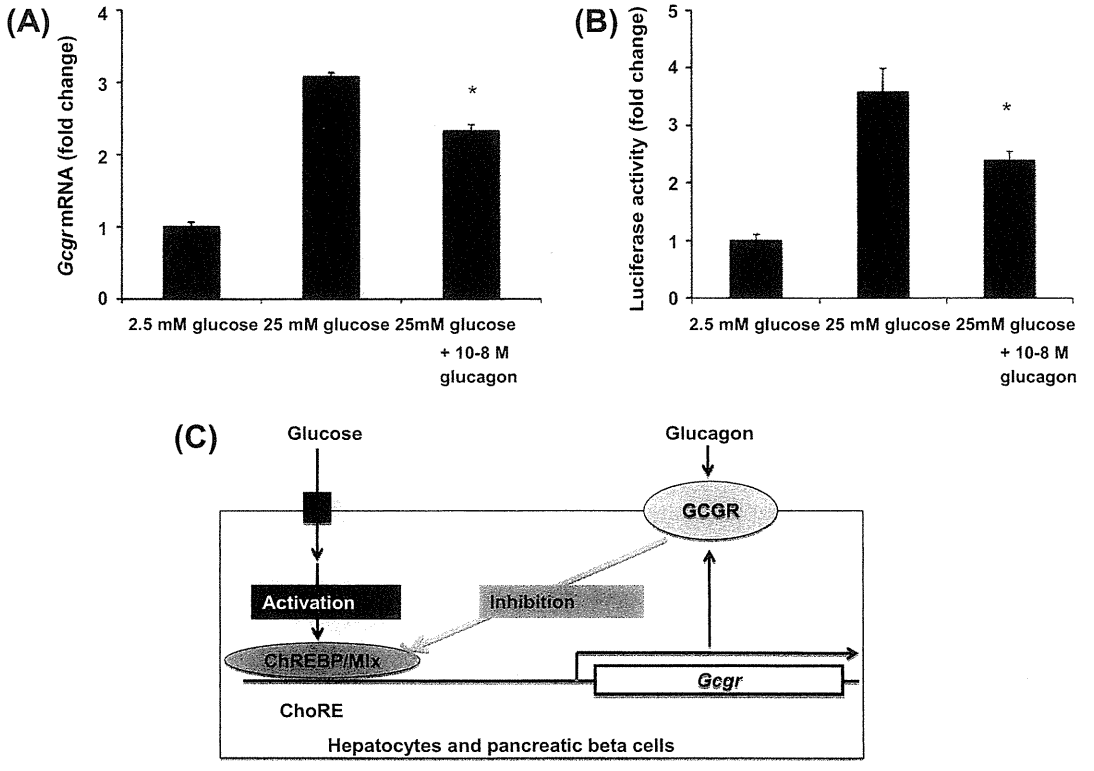

Fig. 4. Glucagon suppresses rat *Gcgr* mRNA expression in INS-1E cells. (A) Addition of 10 nM glucagon partly inhibits glucose-induced *Gcgr* mRNA expression in INS-1E cells. Data represent means ± S.D. ($n = 3$). $^*p < 0.05$ vs. 25 mM glucose. At most points, the error bars are too small to be shown. (B) Addition of 10 nM glucagon partly inhibits glucose-induced luciferase activities in pGL3-ChoRE in INS-1E cells. Data represent means ± S.D. ($n = 6$). $^*p < 0.05$ vs. 25 mM glucose. At most points, the error bars are too small to be shown. (C) Schematic representation of feedback looping between glucose and glucagon signaling in the regulation of *Gcgr* expression.

antibodies showed that ChREBP binds to the region containing ChoRE (Fig. 3C). In contrast, glucose and cotransfection of pcDNA-daChREBP did not increase luciferase activities in the pGL3-G-box (Fig. S3A and S3B). These findings suggest that ChoRE (−554/−538 bp), but not the G-box (−543 bp/−529 bp), is a functional glucose response element.

3.4. Glucagon suppresses ChREBP transactivity in INS-1E cells

In the liver, cAMP activates cAMP-dependent PKA, which in turn inhibits ChREBP transactivity through its phosphorylation. We confirmed that 1 nM of glucagon inhibited glucose-stimulated *Gcgr* gene expression in INS-1E cells (Fig. 4A). In accord with this, glucose-induced luciferase activities in pGL3-ChoRE were partly suppressed by 1 nM glucagon (Fig. 4B). These data suggest a closed feedback loop between glucose and glucagon signaling in the regulation of *Gcgr* expression (Fig. 4C).

4. Discussion

In this study, we found that ChREBP directly regulates rat *Gcgr* mRNA expression by binding to ChoRE in the rat *Gcgr* promoter. Previously, the G-box in the rat *Gcgr* promoter was considered to play a pivotal role in glucose regulation of rat *Gcgr* mRNA expression; however, the results from our reporter and ChIP assays indicate that ChoRE and not the G-box regulates glucose responsiveness on rat *Gcgr* mRNA expression. On the other hand, glucagon inhibits glucose-induced rat *Gcgr* mRNA expression, suggesting a feedback loop system between glucose and glucagon signaling in the regulation of ChREBP target genes such as *Gcgr*.

Glucose induced rat *Gcgr* mRNA expression in INS-1E cells in a dose- and time-dependent manner. This accords with previously reported data [8]. In addition, adenoviral overexpression of daChREBP was found to increase *Gcgr* mRNA expression. Conversely, suppression of ChREBP transactivity by adenovirus expressing dnMlx inhibited glucose-induced *Gcgr* mRNA expression in INS-1E cells. Therefore, glucose stimulation regulates rat *Gcgr* mRNA expression through ChREBP transactivation.

The glucose response element in the rat *Gcgr* promoter was previously known as the G-box [8,22,23]. The sequence of the G-box differs from the consensus recognition sequence of ChoRE (Fig. 2A). The spacing distances between the two E-boxes in the G-box and ChoRE are 3 and 5 bp, respectively (Fig. 2A). From evidence that transcription activity of the glucose response element depends on the spacing distance, we considered that there may be another glucose response element near the G-box in the rat *Gcgr* promoter (Fig. 2A). The consensus sequence for ChoRE (CABGTG-nnCnG-nGnSTG) differs from that of a G-box [20,21]. Interestingly, the ChoRE found in the rat *Gcgr* promoter seems to be a reverse form of the ChoRE motif (CABGTG-nnCnG-nGnSTG). Moreover, deletion studies of the region containing the ChoRE + 6 motifs (−554/−538 bp) show that ChoRE is the minimal functional motif possessing glucose responsiveness. Thus, ChREBP directly regulates rat *Gcgr* mRNA expression through binding to ChoRE (−554/−538 bp).

Glucagon and cAMP inhibit *Gcgr* mRNA expression [24]. Similarly, glucagon and cAMP inhibit ChREBP transactivity through the phosphorylation of cAMP-dependent PKA [10,25]. In accord with these data, our results show that glucagon inhibits *Gcgr* mRNA expression through the inhibition of ChREBP transactivities (Fig. 4A and B). Considered together with glucose-induced *Gcgr* mRNA expression, this suggests that glucose and glucagon

signaling constitutes a closed loop in the regulation of rat *Gcgr* mRNA expression in INS-1E cells (Fig. 4C). Moreover, ChREBP induces transcriptional repressors, such as KLF10 and DEC1, which are regulated by ChREBP itself [14,17]. Furthermore, ChREBP induces hormones with glucose-lowering effects, such as fibroblast growth factor 21 (FGF21) [15], which can suppress ChREBP transactivity by normalizing plasma glucose [26]. Therefore, ChREBP autoregulates its tranactivity by inducing the expression of its target genes, such as *Gcgr*, *Klf10*, *Dec1*, and *Fgf21*.

Under normal conditions, glucagon secretion is suppressed postprandially, and increased during fasting [2–4]. We conclude that increased *Gcgr* mRNA expression during the postprandial state increases glucagon sensitivity in pancreatic β-cells during fasting. Moreover, both hyperglycemia and hyperglucagonemia coexist in both the fasted and the fed state in diabetic patients. Increased *Gcgr* mRNA expression may thus contribute to fasting and postprandial hyperinsulinemia in diabetic patients. Other studies also have found that gene deletion of ChREBP in ob/ob mice prevents glucose intolerance, fatty liver, and diet-induced obesity [13,27]. Inhibition of ChREBP transactivity may thus improve glucose tolerance by decreasing *Gcgr* mRNA expression and glucagon signaling.

In conclusion, we have determined the functions of ChoRE in the rat *Gcgr* promoter. Glucagon inhibits *Gcgr* mRNA expression through inhibition of ChREBP transactivity, and a closed loop system between glucose and glucagon signaling contributes to the prevention of increased glucose-stimulated gene expression. Inhibition of hepatic ChREBP transactivity may thus be an attractive treatment option for metabolic syndrome by decreasing *Gcgr* mRNA expression and subsequent suppression of glucagon effects and de novo lipogenesis.

Acknowledgments

This work was supported by a Grant-in-Aid for Scientific Research from the Japan Society for the Promotion of Science (K. Iizuka), the Kao Research Council for the Study of Healthcare Science (K. Iizuka), and in part by a New Energy and Industrial Technology Development Organization grant (Y. Horikawa).

Appendix A. Supplementary data

Supplementary data associated with this article can be found, in the online version, at doi:10.1016/j.bbrc.2011.12.042.

References

[1] G.M. Reaven, Banting lecture 1988. Role of insulin resistance in human disease, Diabetes 37 (1988) 1595–1607 (Review).
[2] R.A. Rizza, Pathogenesis of fasting and postprandial hyperglycemia in type 2 diabetes: implications for therapy, Diabetes 59 (2011) 2697–2707.
[3] R.H. Unger, L. Orci, Paracrinology of islets and the paracrinopathy of diabetes, Proc. Natl. Acad. Sci. USA 107 (2010) 16009–16012.
[4] D.S. Edgerton, A.D. Cherrington, Glucagon as a critical factor in the pathology of diabetes, Diabetes 60 (2011) 377–380.
[5] P.M. Vuguin, M.J. Charron, Novel insight into glucagon receptor action: lessons from knockout and transgenic mouse models, Diabetes Obes. Metab. 1 (2011) 144–150.
[6] S.L. Conarello, G. Jiang, J. Mu, Z. Li, J. Woods, E. Zycband, J. Ronan, F. Liu, R.S. Roy, L. Zhu, M.J. Charron, B.B. Zhang, Glucagon receptor knockout mice are resistant to diet-induced obesity and streptozotocin-mediated beta cell loss and hyperglycaemia, Diabetologia 50 (2007) 142–150.
[7] H. Sørensen, M.S. Winzell, C.L. Brand, K. Fosgerau, R.W. Gelling, E. Nishimura, B. Ahren, Glucagon receptor knockout mice display increased insulin sensitivity and impaired beta-cell function, Diabetes 55 (2006) 3463–3469.
[8] L. Portois, B. Maget, M. Tastenoy, J. Perret, M. Svoboda, Identification of a glucose response element in the promoter of the rat glucagon receptor gene, J. Biol. Chem. 274 (1999) 8181–8190.
[9] R. Burcelin, C. Mrejen, J.F. Decaux, S.H. De Mouzon, J. Girard, M.J. Charron, In vivo and in vitro regulation of hepatic glucagon receptor mRNA concentration by glucose metabolism, J. Biol. Chem. 273 (1998) 8088–8093.
[10] K. Iizuka, Y. Horikawa, ChREBP: a glucose-activated transcription factor involved in the development of metabolic syndrome, Endocr. J. 55 (2008) 617–624.
[11] K. Iizuka, R.K. Bruick, G. Liang, J.D. Horton, K. Uyeda, Deficiency of carbohydrate response element-binding protein (ChREBP) reduces lipogenesis as well as glycolysis, Proc. Natl. Acad. Sci. USA 101 (2004) 7281–7286.
[12] S. Ishii, K. Iizuka, B.C. Miller, K. Uyeda, Carbohydrate response element binding protein directly promotes lipogenic enzyme gene transcription, Proc. Natl. Acad. Sci. USA 101 (2004) 15597–15602.
[13] K. Iizuka, B. Miller, K. Uyeda, Deficiency of carbohydrate-activated transcription factor ChREBP prevents obesity and improves plasma glucose control in leptin-deficient (ob/ob) mice, Am. J. Physiol. Endocrinol. Metab. 291 (2006) E358–E364.
[14] K. Iizuka, J. Takeda, Y. Horikawa, Krüppel-like factor-10 is directly regulated by carbohydrate response element-binding protein in rat primary hepatocytes, Biochem. Biophys. Res. Commun. 412 (2011) 638–643.
[15] K. Iizuka, J. Takeda, Y. Horikawa, Glucose induces FGF21 mRNA expression through ChREBP activation in rat hepatocytes, FEBS Lett. 583 (2009) 2882–2886.
[16] K. Iizuka, J. Takeda, Y. Horikawa, Hepatic overexpression of dominant negative Mlx improves metabolic profile in diabetes-prone C57BL/6J mice, Biochem. Biophys. Res. Commun. 379 (2009) 499–504.
[17] K. Iizuka, Y. Horikawa, Regulation of lipogenesis via BHLHB2/DEC1 and ChREBP feedback looping, Biochem. Biophys. Res. Commun. 374 (2008) 95–100.
[18] M. Svoboda, L. Portois, W.J. Malaisse, Glucose regulation of the expression of the glucagon receptor gene, Mol. Genet. Metab. 68 (1999) 258–267.
[19] H.M. Shih, Z. Liu, H.C. Towle, Two CACGTG motifs with proper spacing dictate the carbohydrate regulation of hepatic gene transcription, J. Biol. Chem. 270 (1995) 21991–21997.
[20] L. Ma, L.N. Robinson, H.C. Towle, ChREBP*Mlx is the principal mediator of glucose-induced gene expression in the liver, J. Biol. Chem. 281 (2006) 28721–28730.
[21] Y.S. Jeong, D. Kim, Y.S. Lee, H.J. Kim, J.Y. Han, S.S. Im, H.K. Chong, J.K. Kwon, Y.H. Cho, W.K. Kim, T.F. Osborne, J.D. Horton, H.S. Jun, Y.H. Ahn, S.M. Ahn, J.Y. Cha, Integrated expression profiling and genome-wide analysis of ChREBP targets reveals the dual role for ChREBP in glucose-regulated gene expression, PLoS One 6 (2011) e22544.
[22] L. Portois, M. Tastenoy, B. Viollet, M. Svoboda, Functional analysis of the glucose response element of the rat glucagon receptor gene in insulin-producing INS-1 cells, Biochim. Biophys. Acta 1574 (2002) 175–186.
[23] L. Portois, M. Tastenoy, M. Svoboda, Mutational analysis of the glucose regulatory element in the promoter of the glucagon receptor gene, Ann. NY Acad. Sci. 921 (2000) 148–156.
[24] N. Abrahamsen, K. Lundgren, E. Nishimura, Regulation of glucagon receptor mRNA in cultured primary rat hepatocytes by glucose and cAMP, J. Biol. Chem. 270 (1995) 15853–15857.
[25] H. Yamashita, M. Takenoshita, M. Sakurai, R.K. Bruick, W.J. Henzel, W. Shillinglaw, D. Arnot, K. Uyeda, A glucose-responsive transcription factor that regulates carbohydrate metabolism in the liver, Proc. Natl. Acad. Sci. USA 98 (2001) 9116–9121.
[26] S.A. Kliewer, D.J. Mangelsdorf, Fibroblast growth factor 21: from pharmacology to physiology, Am. J. Clin. Nutr. 91 (2010) 254S–257S.
[27] R. Dentin, F. Benhamed, I. Hainault, V. Fauveau, F. Foufelle, J.R. Dyck, J. Girard, C. Postic, Liver-specific inhibition of ChREBP improves hepatic steatosis and insulin resistance in ob/ob mice, Diabetes 55 (2006) 2159–2170.

Diabetol Int (2012) 3:61–64
DOI 10.1007/s13340-011-0052-9

CASE REPORT

Normalization of fasting hyperglycemia is beneficial for successful introduction of small amount of the GLP-1 analog liraglutide in an obese patient with type 2 diabetes mellitus

Katsumi Iizuka · Reiko Tomita · Tetsuya Suwa · Yukio Horikawa · Jun Takeda

Received: 26 August 2011 / Accepted: 18 October 2011 / Published online: 15 November 2011

Abstract A 50-year-old diabetic woman was treated with intensive insulin therapy, but her glycemic levels were very high. After fasting hyperglycemia was normalized by intensive insulin therapy (34 U/day) and administration of 1000 mg metformin and 150 mg miglitol. We introduced liraglutide, a GLP-1 analog, and 0.5 mg glimepiride on day 10. Liraglutide was dosed up to 0.9 mg every 3 days. Metabolic data (fasting glucose, *M* values, plasma C-peptide, proinsulin/plasma C-peptide immunoreactivity ratio, obesity, and plasma leptin) improved after liraglutide administration. Interestingly, subcutaneous injection of only 0.3 mg liraglutide for 3 days augmented glucose-stimulated insulin secretion and the proinsulin-to-CPR ratio, and inhibited plasma leptin concentration. Normalization of fasting hyperglycemia was beneficial for successfully introducing liraglutide in an obese patient with type 2 diabetes mellitus.

Keywords Liraglutide · Glucagon-like-peptide-1 · Type 2 diabetes mellitus · Leptin · Adiponectin

Introduction

Type 2 diabetes mellitus (T2DM) is becoming a social and economic problem worldwide. Intensive insulin therapy (IIT) is a standard therapy for treating T2DM; however, weight gain and severe hypoglycemia are problems when administering IIT to obese patients with T2DM [1]. Incretin-based therapy based on the effect of glucagon-like peptide-1 (GLP-1) is now emerging to overcome this problem [2].

GLP-1 is secreted by intestinal L cells after food intake [3]. It potentiates glucose-stimulated insulin secretion in pancreatic beta cells while suppressing glucagon secretion [3]. In addition, GLP-1 inhibits acid secretion and gastric emptying in the stomach, and reduces food intake by increasing satiety in the brain [3]. Accordingly, GLP-1 therapy reduces plasma glucose concentration without weight gain [2, 3]. Moreover, GLP-1 has a lower risk of causing hypoglycemia because GLP-1 cannot augment insulin secretion when glucose concentrations are normal [3]. The effect of incretin is attenuated in patients with T2DM, primarily because of a reduced insulinotropic effect of gastric inhibitory polypeptide (GIP), whereas the effect of GLP-1 is, relatively, more preserved [2, 3]. The sensitivity of GLP-1 to glucose can be increased to normal levels by infusing a slightly supraphysiological dose of GLP-1. However, the dose–response relationship between GLP-1 and its potentiation of the beta cell response to glucose is impaired in patients with T2DM. Moreover, GLP-1 is easily digested by dipeptidyl peptidase-IV (DPP-IV); however, GLP-1 analogs such as liraglutide and exenatide, which are difficult for DPP-IV to digest, have been developed [2, 3].

This report presents the case of an obese patient with T2DM who underwent successful liraglutide therapy after normalizing plasma glucose concentration by IIT. Interestingly, subcutaneous injection of only 0.3 mg liraglutide for 3 days augmented glucose-stimulated insulin secretion and the proinsulin-to-CPR ratio, and inhibited plasma leptin concentration. Thus, liraglutide is an attractive treatment option for obese patients with T2DM.

Electronic supplementary material The online version of this article (doi:10.1007/s13340-011-0052-9) contains supplementary material, which is available to authorized users.

K. Iizuka (✉) · R. Tomita · T. Suwa · Y. Horikawa · J. Takeda
Department of Diabetes and Endocrinology,
Graduate School of Medicine, Gifu University,
Gifu 501-1194, Japan
e-mail: kiizuka@gifu-u.ac.jp

Case report

A 50-year-old obese woman with T2DM was admitted to the hospital. She was diagnosed with T2DM at the age of 38 years. IIT was started at the age of 40 years; however, her glycemic levels were very high and her average glycosylated hemoglobin (HbA1c (National Glycohemoglobin Standardization Program (NGSP) equivalent value)) level was greater than 10%. Body weight had also increased by 10 kg over 5 years (from 56 to 66.5 kg). She was hospitalized to undergo liraglutide treatment. Before hospitalization, she has been treated with four daily insulin injections (three injections of insulin lispro before breakfast (7 U), lunch (6 U), and dinner (6 U) and one of insulin NPH (20 U) at bedtime) + pioglitazone 7.5 mg/day + miglitol 150 mg/day + metformin 750 mg/day.

Physiological findings on admission

Her height was 153.6 cm and weight was 66.5 kg (body mass index (BMI) 28.2). Resting blood pressure was 111/79 mmHg. No abnormal findings were observed in the thoracoabdominal region. The vibratory sensitivity of the bilateral lower limbs and bilateral ankle reflex had decreased. She had bilateral simple retinopathy.

Laboratory findings

Laboratory data are shown in Supplementary Table S1. No abnormal findings were observed, except glucose (3+) in urinalysis. Blood cell count was normal. Levels of transaminases, creatinine, electrolytes, and blood urea nitrogen (BUN) were within normal ranges. HbA1c level was as high as 11.2% (NGSP equivalent value) and urinary C-peptide level was as low as 44 μg/day. Plasma glucose level at 8:00 and 10:00 am were 180 and 222 mg/dl, respectively. Plasma C-peptide level at 8:00 and 10:00 am were 1.03 and 1.63 ng/ml, respectively. Abdominal computed tomography (CT) revealed diffuse fatty changes in the liver.

Clinical course

Metformin 1000 mg/day, miglitol 150 mg/day, insulin lispro 20 U/day, and insulin NPH 14 U/day were started after hospitalization, in addition to diet therapy (1200 kcal). After we confirmed that the capacity of insulin secretion had decreased but was preserved, and that fasting hyperglycemia at breakfast was normalized, we changed IIT to liraglutide + glimepiride therapy in addition to metformin and miglitol administration (Fig. 1).

After day 16, her appetite was lost, an unpleasant sweet taste was experienced, and metformin and miglitol

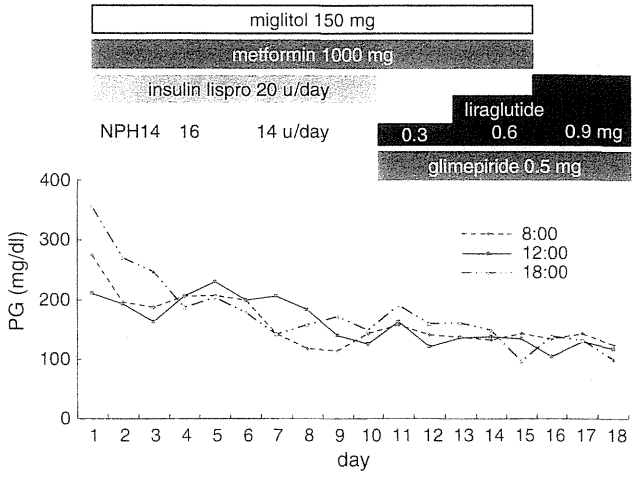

Fig. 1 Clinical course of the patient. Intensive insulin therapy was stopped on day 10, and liraglutide and 0.3 mg glimeperide were started that evening. Liraglutide was dosed up to 0.3 mg every 3 days and continued. Then 150 mg miglitol and 1000 mg metformin was stopped on day 15

administration were stopped; however, her blood glucose did not worsen and these symptoms were improved. Plasma glucose levels at 08:00/10:00/12:00/14:00/18:00/20:00/24:00/03:00 were 180/222/193/186/271/217/257/199 mg/dl, 101/157/164/110/146/192/128/90 mg/dl, and 123/188/130/169/126/150/116/113 mg/ml on days 2, 9, and 18 after hospitalization, respectively (Supplementary Figure S1). M values (M = average ($|10 \times \mathrm{Log}_{10}(\mathrm{BS}/100)|^3$) on days 2, 9, and 18, which reflect blood glucose variations during the day, were 37.3, 5.12, and 4.83, respectively [4]. Plasma C-peptide immunoreactivity (CPR) at 8:00 am/10:00 am on days 2, 9, 12, 15, and 18 was 1.03/1.63, 0.76/1.65, 1.61/2.71, 2.06/2.92, and 2.05/4.14 ng/ml, respectively (Table 1). We measured the proinsulin-to-CPR ratio to evaluate the extent of pancreatic beta cell failure [5]. This ratio on days 9, 12, 15, and 18 was 0.058, 0.031, 0.028, and 0.030, respectively. Thus, pancreatic beta cell failure had improved (Table 1). GLP-1 analogs inhibit postprandial glucagon secretion in vivo [2, 3]. Therefore, we next checked plasma glucagon concentration before and after introducing liraglutide therapy. Plasma glucagon concentrations at 8:00 am/10:00 am on days 2, 9, 12, 15, and 18 were 42/45, 62/61, 24/58, 45/94, and 20/38, respectively (Table 1).

GLP-1 analogs reportedly reduce body weight by reducing appetite [2, 3]. Finally, we checked plasma leptin and adiponectin concentrations in addition to measuring body weight. Body weight on days 2, 9, 12, 15, and 18 was 66.5, 65.5, 64.0, 63.5, and 61.8 kg, respectively (Table 1). Consistent with this result, plasma leptin concentrations on days 9, 12, 15, and 18 were 15.8, 7.5, 6.9, and 6.6 ng/ml, respectively (Table 1). Conversely, plasma adiponectin concentrations on days 9, 12, and 15 were 3.6, 3.5, and 3.1 μg/ml, respectively (Table 1). The patient was

Table 1 The effect of liraglutide on islets function, body weight, and adipokines

	Insulin Day 2		Insulin Day 9		Liraglutide 0.3 mg Day 12		Liraglutide 0.6 mg Day 15		Liraglutide 0.9 mg Day 19	
	8:00	10:00	8:00	10:00	8:00	10:00	8:00	10:00	8:00	10:00
PG (mg/dl)	180	222	101	157	134	152	129	162	123	188
S-CPR (ng/ml)	1.03	1.63	0.76	1.65	1.61	2.71	2.06	2.92	2.05	4.14
Proinsulin (pmol/l)	ND	ND	14.5	ND	16.7	ND	18.8	ND	20.4	ND
Proinsulin/CPR	ND	ND	0.058	ND	0.031	ND	0.028	ND	0.03	ND
Glucagon (pg/ml)	42	45	62	61	24	58	45	94	20	38
Abdominal circumference (cm)	100	ND	97	ND	97	ND	95.2	ND	95	ND
Body weight (kg)	66.45	ND	65.5	ND	64.0	ND	63.5	ND	61.8	ND
Leptin (ng/ml)	ND	ND	15.8	ND	7.5	ND	6.9	ND	6.6	ND
Adiponectin (μg/ml)	ND	ND	3.6	ND	3.5	ND	3.1	ND	ND	ND

subsequently discharged from the hospital on day 19. One month after discharge, her HbA1c level had improved to 8.2% (NGSP equivalent value).

Discussion

In this case, we observed that normalizing fasting hyperglycemia is important to introducing liraglutide therapy. Moreover, administration of only 0.3 mg liraglutide was sufficient to improve plasma glucose, augment glucose-stimulated insulin secretion, improve pancreatic beta cell failure, and reduce plasma leptin concentration.

We hypothesized that it was important to normalize fasting hyperglycemia to successfully introduce liraglutide therapy. The supporting evidence is:

1. increasing fasting plasma glucose concentration causes a decrease in glucose augmentation of insulin secretion [6];
2. restoration of normoglycemia with insulin in patients with T2DM improves beta cell function [7, 8];
3. normalizing hyperglycemia partly restores reduced GLP-1 and GIP receptor expression in pancreatic beta cells [9, 10]; and
4. 4-week normalization of plasma glucose level improves GLP-1 and GIP sensitivity in pancreatic beta cells in humans [11, 12].

To maintain fasting normoglycemia, we administered 0.5 mg glimepiride in the evening and metformin at bedtime rather than insulin NPH at bedtime to suppress hepatic gluconeogenesis through the night; plasma glycemic control was stable throughout liraglutide treatment. Thus, normalizing fasting hyperglycemia is beneficial for introducing liraglutide therapy.

Liraglutide is known to improve proinsulin-to-CPR ratio and fasting CPR/FPG ratio [13]. Consistent with these results, liraglutide successfully improved proinsulin-to-CPR ratio and CPR index in our patient also. Conversely, glimepiride increases both CPR and proinsulin secretion, and worsens beta cell function (proinsulin/insulin ratio) [14]. Ideally, combination therapy of long acting insulin and liraglutide will be more beneficial for this patient.

Excess glucagon secretion is important in promoting both basal and postprandial hyperglycemia in patients with T2DM [3, 15]. Some groups have shown an inhibitory effect of GLP-1 on glucagon release in patients with T2DM and in patients with type 1 diabetes [13, 16]. In contrast, we found that liraglutide treatment had no effect on the fasting and postprandial glucagon concentrations in our patient. Thus, a higher concentration of GLP-1 may have been necessary to suppress glucagon secretion in our patient.

Whether GLP-1 receptors occur in adipose tissue is still controversial [3]. Expression of the GLP-1 receptor in adipose tissue is absent or very low [17], whereas GLP-1 induces adiponectin mRNA expression in 3T3L1 adipocytes [18]. GLP-1 reduces body weight and plasma leptin concentration in obese mice [19]. In our patient, plasma leptin concentration decreased immediately after liraglutide treatment. Similarly, plasma adiponectin concentration decreased. Subsequently, her appetite remained suppressed and body weight decreased. Although the precise mechanism of how GLP-1 suppresses leptin secretion is still unknown, liraglutide is effective for reducing body weight and appetite.

In this case, administration of only 0.3-mg liraglutide was sufficient to improve plasma glucose and beta cell function. In Japanese patients with T2DM, 0.1, 0.3, 0.6, and 0.9 mg liraglutide dose-dependently reduced HbA1c versus placebo by 0.79, 1.22, 1.64 and 1.85%, respectively [20]. In Caucasians, 1.2 and 1.8 mg liragulutide was used. GLP-1 sensitivity in Japanese patients may be much better than in Caucasian patients.

In conclusion, we report a patient for whom liraglutide effectively improved glycemic control similar to IIT. Normalizing fasting hyperglycemia is beneficial for successful introduction of the GLP-1 analog liraglutide in patients with T2DM.

Conflict of interest The authors state that they have no conflict of interest.

References

1. Wajchenberg BL. Beta-cell failure in diabetes and preservation by clinical treatment. Endocr Rev. 2007;28:187–218.
2. Nauck MA. Incretin-based therapies for type 2 diabetes mellitus: properties, functions, and clinical implications. Am J Med. 2011;124:S3–18.
3. Holst JJ. The physiology of glucagon-like peptide 1. Physiol Rev. 2007;87:1409–39.
4. Wójcicki JM. Mathematical descriptions of the glucose control in diabetes therapy. Analysis of the Schlichtkrull "M"-value. Horm Metab Res. 1995;27:1–5.
5. Inoguchi T, Umeda F, Kakimoto M, Sako Y, Ishii H, Noda K, Kunisaki M, Imamura M, Yu HY, Etoh T, Yoshikawa H, Aoki T, Hashimoto T, Nawata H. Chronic sulfonylurea treatment and hyperglycemia aggravate disproportionately elevated plasma proinsulin levels in patients with type 2 diabetes. Endocr J. 2000;47:763–70.
6. Coates PA, Ollerton RL, Luzio SD, Ismail I, Owens DR. A glimpse of the 'natural history' of established type 2 (non-insulin dependent) diabetes mellitus from the spectrum of metabolic and hormonal responses to a mixed meal at the time of diagnosis. Diabetes Res Clin Pract. 1994;26:177–87.
7. Yoshioka N, Kuzuya T, Matsuda A, Iwamoto Y. Effects of dietary treatment on serum insulin and proinsulin response in newly diagnosed NIDDM. Diabetes. 1989;38:262–6.
8. Laedtke T, Kjems L, Pørksen N, Schmitz O, Veldhuis J, Kao PC, Butler PC. Overnight inhibition of insulin secretion restores pulsatility and proinsulin/insulin ratio in type 2 diabetes. Am J Physiol Endocrinol Metab. 2000;279:E520–8.
9. Lynn FC, Pamir N, Ng EH, McIntosh CH, Kieffer TJ, Pederson RA. Defective glucose-dependent insulinotropic polypeptide receptor expression in diabetic fatty Zucker rats. Diabetes. 2001;50:1004–11.
10. Xu G, Kaneto H, Laybutt DR, Duvivier-Kali VF, Trivedi N, Suzuma K, King GL, Weir GC, Bonner-Weir S. Downregulation of GLP-1 and GIP receptor expression by hyperglycemia: possible contribution to impaired incretin effects in diabetes. Diabetes. 2007;56:1551–8.
11. Højberg PV, Vilsbøll T, Rabøl R, Knop FK, Bache M, Krarup T, Holst JJ, Madsbad S. Four weeks of near-normalisation of blood glucose improves the insulin response to glucagon-like peptide-1 and glucose-dependent insulinotropic polypeptide in patients with type 2 diabetes. Diabetologia. 2009;52:199–207.
12. Højberg PV, Zander M, Vilsbøll T, Knop FK, Krarup T, Vølund A, Holst JJ, Madsbad S. Near normalisation of blood glucose improves the potentiating effect of GLP-1 on glucose-induced insulin secretion in patients with type 2 diabetes. Diabetologia. 2008;51:632–40.
13. Degn KB, Juhl CB, Sturis J, Jakobsen G, Brock B, Chandramouli V, Rungby J, Landau BR, Schmitz O. One week's treatment with the long-acting glucagon-like peptide 1 derivative liraglutide (NN2211) markedly improves 24-h glycemia and alpha- and beta-cell function and reduces endogenous glucose release in patients with type 2 diabetes. Diabetes. 2004;53:1187–94.
14. van der Wal PS, Draeger KE, van Iperen AM, Martini C, Aarsen M, Heine RJ. Beta cell response to oral glimepiride administration during and following a hyperglycaemic clamp in NIDDM patients. Diabet Med. 1997;14:556–63.
15. Rizza RA. Pathogenesis of fasting and postprandial hyperglycemia in type 2 diabetes: implications for therapy. Diabetes. 2010;59:2697–707.
16. Kielgast U, Holst JJ, Madsbad S. Antidiabetic actions of endogenous and exogenous GLP-1 in type 1 diabetic patients with and without residual β-cell function. Diabetes. 2011;60:1599–607.
17. Bullock BP, Heller RS, Habener JF. Tissue distribution of messenger ribonucleic acid encoding the rat glucagon-like peptide-1 receptor. Endocrinology. 1996;137:2968–78.
18. Kim Chung le T, Hosaka T, Yoshida M, Harada N, Sakaue H, Sakai T, Nakaya Y. Exendin-4, a GLP-1 receptor agonist, directly induces adiponectin expression through protein kinase A pathway and prevents inflammatory adipokine expression. Biochem Biophys Res Commun. 2009;390:613–8.
19. He M, Su H, Gao W, Johansson SM, Liu Q, Wu X, Liao J, Young AA, Bartfai T, Wang MW. Reversal of obesity and insulin resistance by a non-peptidic glucagon-like peptide-1 receptor agonist in diet-induced obese mice. PLoS One. 2010;5:e14205.
20. Seino Y, Rasmussen MF, Zdravkovic M, Kaku K. Dose-dependent improvement in glycemia with once-daily liraglutide without hypoglycemia or weight gain: a double-blind, randomized, controlled trial in Japanese patients with type 2 diabetes. Diabetes Res Clin Pract. 2008;81:161–8.

日本臨牀　70巻 増刊号3（2012年5月20日発行）別刷

最新臨床糖尿病学 上

—糖尿病学の最新動向—

IV. 糖尿病の疾患概念・病型分類・成因

その他の特定の機序・疾患による糖尿病

遺伝子異常が同定されている糖尿病

堀川幸男

IV 糖尿病の疾患概念・病型分類・成因

その他の特定の機序・疾患による糖尿病

遺伝子異常が同定されている糖尿病

Monogenic diabetes in children and young adults

堀川幸男

Key words：新生児糖尿病，遺伝子異常，インスリン分泌不全，MODY

はじめに

‘遺伝子異常による糖尿病’とは糖尿病の成因分類の‘III．その他の特定の機序，疾患によるもの’のうち，‘A．遺伝因子として遺伝子異常が同定されたもの’と，‘B-⑦ その他の遺伝的症候群で糖尿病を伴うことの多いもの’の一部が含まれる．糖尿病全体の数％を占めるにすぎないが，コモン2型糖尿病の病態解明のヒントを与える可能性もあり原因遺伝子の同定が進められてきた．原因遺伝子を同定することにより，その糖尿病の病型を正確に診断できるうえに，病態にあった治療法を選択することができ，予後の改善にもつながる．

本稿では，糖尿病を発症する単一遺伝子疾患について，肥満や脂肪萎縮を合併するものも含め解説する．

1 膵β細胞機能にかかわる遺伝子異常

1）インスリン分泌不全型を呈する遺伝子異常

新生児糖尿病（NDM）は生後6カ月未満に発症する糖尿病の総称で，高血糖やケトアシドーシスの発症を契機に発見され，インスリン治療を必要とすることが多い（**表1**）．約半数は生涯続く永続型（permanent neonatal diabetes mellitus: PNDM）であるが，残りの半数は主に生後1年以内に寛解する一過性型（transient neonatal diabetes mellitus: TNDM）である[1]．TNDMの40％は後に再発し，2型糖尿病の表現型を示す．臨床像からPNDMとTNDMを区別することは難しく，治療法の選択，予後の推測および遺伝カウンセリングにとって遺伝子検査は必須である．最初に述べる3つの遺伝子はNDMの原因として大きな割合を占めるものである．

a. INS遺伝子異常

糖尿病の発症年齢は新生児期から小児期，成人期にわたる．高IRI血症の場合は加齢など環境要因が加わり糖尿病が発症する型であるが，新生児発症型では遺伝子変異により，プロインスリンのミスフォールディングから小胞体ストレスがたまりβ細胞不全をきたしアポトーシスに至ると考えられている．多くは常染色体優性でPNDMの表現型を呈するが[2]，MODY（maturity-onset diabetes of the young）（MODY10）の報告もある．高IRI血症を示す症例だけでなく，MODY様あるいは自己抗体陰性で家族歴濃厚な1型糖尿病様の症例（type 1B）においては，インスリン遺伝子異常を疑いシークエンスを施行すべきである．日本人NDMにおけるインスリン遺伝子の詳細な頻度解析の報告はまだない．

Yukio Horikawa: Department of Diabetes and Endocrinology, Division of Molecule and Structure, Gifu University School of Medicine 岐阜大学大学院医学系研究科 内分泌代謝病態学

0047-1852/12/¥60/頁/JCOPY

表1 新生児糖尿病の原因遺伝子リスト

遺伝子/染色体	PNDM/TNDM	遺伝形式	糖尿病以外の特徴
β細胞機能の低下			
KCNJ11/ABCC8	PNDM/TNDM	常優 or 常劣	発達遅延，てんかん
Chr.6q24	TNDM	様々	巨舌，臍帯ヘルニア
GCK	PNDM	常劣	両親が*GCK*ヘテロ変異による高血糖
SLC2A2	PNDM	常優	高ガラクトース血症，肝不全
GLIS3	PNDM	常劣	先天性甲状腺機能低下，緑内障，肝硬変，cystic kidney
NEUROD1	PNDM	常劣	小脳低形成，感音難聴，強度の近視，網膜低形成
PAX6	PNDM	常劣	小頭症，小眼症，汎下垂体機能低下症
膵低形成			
PTF1A	PNDM	常劣	膵臓および小脳の無形成
PDX1	PNDM	常劣	膵臓の無形成
HNF1B	PNDM/TNDM	常優	膵外分泌低下，腎嚢胞
NEUROG3	PNDM	常劣	先天性下痢，腸内分泌細胞欠失
RFX6	PNDM	常劣	小腸閉鎖，胆嚢低形成，下痢
β細胞破壊の増加			
EIF2AK3	PNDM	常劣	脊椎骨端の低形成，腎不全，繰り返す肝炎，精神発達遅延
FOXP3	PNDM	X染色体	免疫不全，難治性下痢，湿疹様皮疹，IgE高値
INS	PNDM	常優	なし
IER3IP1	PNDM	常劣	小脳症，重度小児てんかん性脳症

b. KCNJ11/ABCC8遺伝子異常

大部分の症例は孤発でその他は常染色体優性である．遺伝子異常の種類により，PNDMからMODY様のものまで様々な表現型をとるが，KCNJ11遺伝子異常ではPNDMが多く，ABCC8遺伝子異常ではTNDMが多い．スルホニルウレア薬(SU薬)が効を奏するが，必要量は通常の2型糖尿病で使用する場合よりも多い．20–25％にてんかん，発達遅延などの神経学的症候を合併するので(DEND syndrome; developmental delay, epilepsy, neonatal diabetes)，これに対するSU薬の効果についても検討が待たれる．コーカソイドの報告では，PNDMの原因の約半数はKATPチャネルを構成するKCNJ11(Kir6.2)とABCC8(SUR1)サブユニットの遺伝子異常である．残りのうち15–20％はINS遺伝子異常で他はまれである[3]．

c. 6q24領域の異常(TNDM1)

3種類の型の異常(父親由来のダイソミー，父親由来の6q24領域の重複，母親由来の第6番染色体のメチル化異常)があり，それによる父親由来のZAC/PLAGL1(zinc finger protein regulating apoptosis and cell cycle arrest; PACAPの1型受容体の転写調節因子)とHYMAI(hydatidiform mole associated and imprinted gene; untranslated mRNA)の過剰発現が原因である．また母親由来の第6番染色体のメチル化異常には，ZFP57遺伝子が常染色体劣性形式で関与しているといわれている．TNDMの大部分が6q24領域のインプリンティング異常に由来し，KCNJ11とABCC8の異常も一部存在する．日本人新生児糖尿病の遺伝子異常の報告でも，同様の傾向が認められている[4]．

d. MODY遺伝子異常

MODYの主たる病態は膵β細胞のインスリン分泌不全であるが，遺伝様式と発症年齢を除けば，MODYは‘やせ型インスリン分泌不全’を特徴とするコモン日本人2型糖尿病と類似した臨床像を呈する．そこで，その原因遺伝子が調べられた結果，現在までに6種類の主たる原因遺伝子(MODY1–6)が同定されている．なおMODY7–11は非常にまれと考えられている(表

表2 既知MODYの原因遺伝子と特徴

	遺伝子名	平均診断時年齢	特徴的臨床像	治療
MODY1	*HNF4A*	17(5-18)	MODY3と類似 他に巨大児，低HDL血症，一過性新生児低血糖	少量SU薬
MODY2	*GCK*	10(0-18)	空腹時血糖値の軽微な上昇 妊娠糖尿病の5％	無治療
MODY3	*HNF1A*	14(4-18)	尿糖の閾値が低い→学校検尿で指摘されることあり 合併症の進行は1型や2型と同じ	SU薬によく反応
MODY4	*PDX1*	(3家系のみ)	ホモでPNDM，膵外分泌不全，膵の無形成．ヘテロではIGT～DMまで様々	食事療法～インスリン
MODY5	*HNF1B*	21(0-73)	腎嚢胞，腎異形成，性腺形成異常，膵低形成，肝機能異常，高尿酸血症など	食事療法～インスリン
MODY6	*NEUROD1*	(5家系のみ)	発症年齢や糖尿の重症度，合併症の進行などの表現型は様々	食事療法～インスリン
MODY7	*KLF11*	(3家系のみ)	酸化ストレスに対するβ細胞の感受性亢進？ *PDX1*の発現を調節？	無治療～インスリン
MODY8	*CEL*	(2家系のみ)	膵外分泌機能低下，軽度の腹痛，軟便，膵臓の線維化，萎縮	経口薬 インスリン
MODY9	*PAX4*	(2家系のみ)	軽症～進行した腎症まであり	食事療法 経口薬
MODY10	*INS*	11週(0-23歳)	新生児糖尿病では頻度が高いが，MODYとしてはまれ．自己抗体陰性の1型糖尿病でみられることがある	インスリン
MODY11	*BLK*	(1家系のみ)	肥満が発症を修飾	食事療法～インスリン

2)．MODY1-6のうち，MODY2以外は転写因子の異常である．我が国ではMODY3が最も多く，その他のMODYはまれとされてきたが，著者らのスクリーニングでは，MODY2はそれほどまれではないことが判明している(未発表データ)．MODY2は一般に軽症であり空腹時の軽い高血糖や耐糖能異常のみで，糖尿病を発症するのは50％以下である．しかし，今後，グルコキナーゼ活性化薬の導入も予想され，本遺伝子変異の検索は，薬剤応答性を判断するうえで重要である．MODY3ではSU薬が効果的であり，多くの症例でインスリンからの切り替えが可能である．MODY5(RCAD: renal cysts and diabetes syndrome)ではHNF1β遺伝子の大規模遺伝子欠損による場合が40％と高率に認められ，直接シークエンスを第一選択としては見落とすので注意が必要である．また進行性の腎機能障害，腎嚢胞，腎低形成や奇形などを伴い，糖尿病の発症よりも先に認識されることも多い．なお原因遺伝子が不明のMODY(MODY-X)は，我が国では80％，欧米では20-30％を占めており，新規原因遺伝子同定が待たれる[5]．

e. ミトコンドリア糖尿病

mtDNA変異により，糖尿病以外に感音性難聴，脳筋症および心筋症などが認められる．3243点変異は日本人糖尿病患者の1％に認められ最も高頻度であり，低身長，痩せ型，30歳代発症および90％に感音性難聴などの臨床像がみられる．インスリン分泌は進行性に低下し，糖尿病合併症も進行しやすく，血中乳酸値は高値を示す[6]．

2) インスリン作用の伝達機構にかかわる遺伝子異常

a. インスリン受容体遺伝子異常

インスリン受容体(INSR)異常症は，常染色体劣性型が多く，同じインスリン受容体異常でも表現型の違いにより3種類に分けられる．インスリン受容体異常症A型，Rabson-Mendenhall症候群，妖精症(leprechaunism)の順に重症

化する．妖精症では子宮内発育不全，鞍鼻，空腹時低血糖，皮下脂肪の減少，陰核肥大を認め1歳未満で死亡する．Rabson-Mendenhall症候群はより軽症であり，発達遅延や歯牙異常を認め，青年期までに死亡することが多い．インスリン受容体異常症A型は最も軽症で発症が成年期と遅い．大量のインスリン投与でもコントロール困難な症例に対し，インスリンと50％の類似性をもつIGF-Iの投与が行われる．肥満を伴わない表皮黒色腫，高インスリン血症，高アンドロゲン血症を共通して認める[7]．

2 その他の遺伝的症候群で糖尿病を伴うことの多いもの

1）インスリン分泌不全型を呈する遺伝的症候群

a. Wolfram症候群

糖尿病以外に視神経萎縮，難聴，尿崩症を伴い，DIDMOAD症候群(diabetes insipidus, diabetes mellitus, optic atrophy and deafness)とも呼ばれ，平均寿命は30歳とされる．常染色体劣性遺伝であり，90％以上がWFS遺伝子異常である．糖尿病治療は，発症時よりインスリンが必要である[8]．

b. Wolcott-Rallison症候群(WRS)

WRSはまれな常染色体劣性遺伝性疾患であり，多くは生後6カ月くらいに突然インスリン依存型糖尿病で発症する．低身長を主徴として，加齢とともに骨折，肝脾腫，腎障害，精神発達遅延，心血管異常などの症状が認められる．原因はタンパク翻訳調節因子のEIF2AK3であることが判明しており，膵β細胞のアポトーシスなどを介して糖尿病発症にかかわっていると考えられている[9]．

c. Roger症候群(thiamine-responsive megaloblastic anemia: TRMA症候群)

サイアミントランスポーターをコードするSLC19A2遺伝子異常による常染色体劣性遺伝形式をとるまれな疾患で，小児期発症の糖尿病，貧血，感音性難聴を特徴とする[10]．

d. IPEX症候群(immune dysregulation, polyendocrinopathy, enteropathy, X-linked)

FOXP3遺伝子異常による伴性劣性遺伝形式の疾患で，免疫調節異常・多発性内分泌障害・腸症などが認められる．変異を受け継いだ男子のみが，致死性の自己免疫性・炎症性・アレルギー性免疫疾患を発症する．膵臓，甲状腺，大腸，皮膚など様々な臓器に炎症・組織破壊が起こり，通常生後1，2年以内に死亡する[11]．

2）インスリン抵抗性型を呈する遺伝的症候群

a. 先天性脂肪過多疾患

a）Alstrom症候群

小児期からの肥満を特徴とする常染色体劣性疾患であり，インスリン抵抗性型糖尿病，脂質異常症，網膜色素変性および難聴などの知覚神経異常を呈する．一般に精神遅滞や性腺の発育遅延は認められない．原因遺伝子はALMS1遺伝子が同定されているが，ホルモン感受性調節にかかわっている可能性がいわれている[12]．

b）Bardet-Biedl症候群

小児期からの肥満を特徴とするが，特に内臓脂肪蓄積が顕著であり，高血圧と糖尿病以外に，精神遅滞と性腺の発育遅滞，四肢の形態異常，網膜変性および腎臓の形態・機能異常などがよく認められる．原因遺伝子座は少なくとも8カ所以上存在することが判明しており，BBS1，BBS2，BBS4の異常でほとんどの症例が説明される．機能はまだ不明な部分が多いが，神経細胞などの繊毛運動機能に関係するといわれている[13]．

c）Prader-Willi症候群

新生児期の筋緊張低下，精神発達遅滞，食欲亢進による肥満，視床下部性内分泌異常などが認められる疾患で，原因は第15番染色体15q11-13の刷り込み領域の異常が同定されている．原因遺伝子としてnecdinなどが考えられている[14]．

他にレプチンやレプチン受容体の遺伝子変異から著明な肥満を介して高率に糖尿病を発症するが，ここでは省略する．またDown症候群，

Turner症候群，Klinefelter症候群などの染色体異常，筋強直性ジストロフィーなども肥満あるいは筋肉減少からインスリン抵抗性を介して糖尿病を発症することが多い．

b. 先天性脂肪萎縮症

インスリン抵抗性と重度の脂質異常症，脂肪肝を認める場合には，一度は考慮すべき疾患である．遺伝学的に不均一でまれな疾患で，部分的あるいは全身性の皮下脂肪組織を欠損する．

a）部分型脂肪萎縮症

常染色体優性の部分型脂肪萎縮症が最も多く，核膜成分を構成するlamin A/CをコードするLMNA遺伝子異常が原因とされている．生下時の皮下脂肪は正常であるが，思春期になると四肢と体幹の皮下脂肪萎縮が明瞭となる．いまだ機能的に不明な点も多いが，LMNA遺伝子が筋・脂肪細胞のアポトーシスに関与している可能性がいわれている[15]．

b）全身性脂肪萎縮症

常染色体劣性の全身性脂肪萎縮症（Berardinelli-Seip症候群）のうち，BSCL1（AGPAT2）とBSCL2（Seipin）異常が95％以上を占めるが，臨床的な区別は困難である．AGPAT2の低下によりIL-6やTNF-αの発現が脂肪組織で亢進することが報告されている[15]．Seipinはリン脂質の代謝に関係しているとの報告があるが，まだ不明な点も多い．肝腫大が多く，先端巨大症様の顔貌がみられることもあり，糖尿病は20歳までに発症することが多い．

その他，PPARγの優性阻害型変異や老化症候群であるWerner症候群でも脂肪萎縮からインスリン抵抗性の亢進が認められているが，詳細はここでは省略する．

3）どちらにも分けられないもの

a. Fanconi-Bickel症候群

常染色体劣性遺伝性疾患であり，肝臓および腎臓におけるグリコーゲンの過剰蓄積，近位尿細管障害，グルコースとガラクトースの利用障害が特徴的である．原因は糖輸送体であるGLUT2（SLC2A2）であることが判明しており，空腹時の低血糖と対照的に食後は，グルコース応答性インスリン分泌の低下と肝臓への糖の取り込みが阻害されるため，著明な高血糖が認められる．治療としてはGLUT5が輸送体であるフルクトースを単純糖質として摂取する[16]．

おわりに

本稿では主に単一遺伝子の配列異常で糖尿病発症が説明されている例を紹介したが，今後は，CNVなどの遺伝子の構造変異やエピジェネティクスを含めて原因遺伝子探索を進めねばならないことも疑いなく，これにより初めて糖尿病の遺伝素因の全貌を明らかにすることができると考える．

文 献

1) Greeley SA, et al: Neonatal diabetes: an expanding list of genes allows for improved diagnosis and treatment. Curr Diabetes Rep **11**: 519-532, 2011.
2) Edghill EL, et al: Insulin mutation screening in 1,044 patients with diabetes: mutations in the INS gene are a common cause of neonatal diabetes but a rare cause of diabetes diagnosed in childhood or adulthood. Diabetes **57**: 1034-1042, 2008.
3) Murphy R, et al: Clinical implications of a molecular genetic classification of monogenic β-cell diabetes. Nat Clin Prac Endocrinol Metab **4**: 200-213, 2008.
4) Suzuki S, et al: Molecular basis of neonatal diabates in Japanese patients. J Clin Endocrinol Metab **92**: 3979-3985, 2007.
5) Fajans SS, Bell GI: MODY: history, genetics, pathophysiology, and clinical decision making. Diabetes Care **34**: 1878-1884, 2011.
6) Suzuki S: Diabetes mellitus with mitochondrial gene mutations in Japan. Ann N Y Acad Sci **1011**: 185-192, 2004.
7) Longo N, et al: Genotype-phenotype correlation in inherited severe insulin resistance. Hum Mol Genet **11**: 1465-1475, 2002.

8) Rohayem J, et al: Diabetes and neurodegeneration in Wolfram syndrome: a multicenter study of phenotype and genotype. Diabetes Care **34**: 1503-1510, 2011.
9) Rubio-Cabezas O, et al: Wolcott-Rallison syndrome is the most common genetic cause of permanent neonatal diabetes in consanguineous families. J Clin Endocrinol Metab **94**: 4162-4170, 2009.
10) Bergmann AK, et al: Thiamine-responsive megaloblastic anemia: identification of novel compound heterozygotes and mutation update. J Pediatr **155**: 888-892.e1, 2009.
11) Rubio-Cabezas O, et al: Clinical heterogeneity in patients with FOXP3 mutations presenting with permanent neonatal diabetes. Diabetes Care **32**: 111-116, 2009.
12) Girard D, Petrovsky N: Alström syndrome: insights into the pathogenesis of metabolic disorders. Nat Rev Endocrinol **7**: 77-88, 2011.
13) Zaghloul NA, Katsanis N: Mechanistic insights into Bardet-Biedl syndrome, a model ciliopathy. J Clin Invest **119**: 428-437, 2009.
14) Aebischer J, et al: Necdin protects embryonic motoneurons from programmed cell death. PLoS One **6**: e23764, 2011.
15) Capeau J, et al: Human lipodystrophies: genetic and acquired diseases of adipose tissue. Endocr Dev **19**: 1-20, 2010.
16) Taha D, et al: Hyperglycemia and hypoinsulinemia in patients with Fanconi-Bickel syndrome. J Pediatr Endocrinol Metab **21**: 581-586, 2008.

Journal of Diabetes and Its Complications 26 (2012) 113–117

Contents lists available at SciVerse ScienceDirect

Journal of Diabetes and Its Complications

journal homepage: WWW.JDCJOURNAL.COM

Associations of plasma von Willebrand factor ristocetin cofactor activity and 5-hydroxyindole acetic acid concentrations with blood flow in lower-leg arteries in Japanese type 2 diabetic patients with normal ankle-brachial index

Hiroshi Murase[a], Eiji Suzuki[b,*], Yoshitaka Tajima[b], Kanako Hayashi[b], Tomohiko Nakamura[b], Nobuyasu Noritake[a], Jun Takeda[c]

[a] Department of Internal Medicine, Daiyukai General Hospital, 1-9-9 Sakura, Ichinomiya, Aichi 491-8551, Japan
[b] Department of Diabetes and Endocrinology, Gifu Prefectural General Medical Center, 4-6-1 Noishiki, Gifu, Gifu 500-8717, Japan
[c] Department of Diabetes and Endocrinology, Gifu University School of Medicine, 1-1 Yanagido, Gifu, Gifu 501-1194, Japan

ARTICLE INFO

Article history:
Received 8 May 2011
Accepted 17 February 2012
Available online 28 March 2012

Keywords:
Type 2 diabetes
Peripheral circulation
Arterial stiffness
Vascular resistance
Endothelial factors

ABSTRACT

Aims: To evaluate the associations of circulating levels of proinflammatory molecules and endothelial factors with blood flow in lower-leg arteries in diabetic patients with normal ankle-brachial index (ABI>0.9).
Methods: We enrolled 123 type 2 diabetic patients with normal ABI and 30 age-matched nondiabetic subjects consecutively admitted to our hospital. Flow volume and resistive index, an index of peripheral vascular resistance, at the popliteal artery were evaluated using gated two-dimensional cine-mode phase-contrast magnetic resonance imaging. An automatic device was used to measure ABI and brachial-ankle pulse-wave velocity (baPWV) for evaluation of arterial stiffness. Plasma soluble intercellular adhesion molecule-1 (sICAM-1) and monocyte chemoattractant protein-1 (MCP-1) concentrations, serum high-sensitivity C-reactive protein (hsCRP) levels, plasma von Willebrand factor ristocetin cofactor activity (VWF), and plasma vasoconstrictor serotonin metabolite 5-hydroxyindole acetic acid (5-HIAA) concentrations were measured.
Results: Diabetic patients had higher baPWV ($P<.0001$), resistive index ($P<.0001$), sICAM-1 ($P<.0001$), MCP-1 ($P=.0224$), log hsCRP ($P<.0001$), VWF ($P<.0001$), 5-HIAA ($P=.0015$), and lower blood flow ($P<.0001$) than nondiabetic subjects. VWF ($P=.0019$) or 5-HIAA ($P=.0011$), but not sICAM-1, MCP-1, and log hsCRP, was negatively correlated with blood flow in diabetic patients. A multivariate analysis revealed that the significant independent determinants of blood flow were hypertension, use of renin–angiotensin system inhibitors, VWF and 5-HIAA ($r^2=0.198$, $P<.0001$) in diabetic patients.
Conclusions: Plasma VWF and 5-HIAA concentrations are associated with blood flow and are involved in the pathogenesis of impaired peripheral circulation due to higher arterial stiffness and greater vascular resistance in lower-leg arteries in diabetic patients with normal ABI.

1. Introduction

Lower-extremity arterial disease is a major cause of ischemic limb, foot ulcers, and leg amputation in diabetic patients (Faglia et al., 2009; Gorogawa et al., 2006). Diabetic patients are known to have two distinct types of insufficient arterial blood flow to the lower limbs associated with the vessel wall properties. The diabetic condition promotes atherosclerotic plaque formation in the vessel wall and leads to peripheral artery disease (PAD), resulting in reduced blood supply to lower limbs during exercise or at rest. To help identify high-risk patients with PAD, the ankle-brachial index (ABI) is generally used (American Diabetes Association, 2003). The diabetic condition also causes higher arterial rigidity and greater vascular resistance to blood flow, resulting in reduced blood supply in the lower-leg arteries even though the individual has a normal ABI (> 0.9) (Suzuki et al., 2001). It has been reported that waveform analysis at the popliteal artery provides a powerful tool for identifying impaired peripheral circulation caused by either occlusive arterial disease or increased arterial stiffness and peripheral vascular resistance in diabetic patients using gated two-dimensional cine-mode phase-contrast magnetic resonance imaging (2D-cine-PC MRI) (Suzuki et al. 2001). In Japanese patients with diabetes, elderly patients (>65 years) had a higher prevalence of PAD (12.7%) compared with younger patients (<65 years) (4.0%) (Maeda et al., 2008). Prevalence of diabetic patients with low ABI (<0.90) and intermittent claudication is similar to that of diabetic patients with normal ABI and reduced blood flow in lower-leg arteries, indicating that increase in arterial stiffness and vascular resistance to blood flow may be one of the major causes of lower-extremity arterial disease in Japan (Suzuki et al., 2003).

* Corresponding author. Tel.: +81 58 246 1111; fax: +81 58 248 3805.
E-mail address: esuzuki@gifu-hp.jp (E. Suzuki).

1056-8727/$ – see front matter © 2012 Elsevier Inc. All rights reserved.
doi:10.1016/j.jdiacomp.2012.02.003